Supramolecular Regulation of Photophysical Properties and Electron Paramagnetic Resonance Studies of Novel Rod−Coil Ordered Copolymers Based on Poly(*p*-phenylene benzobisoxazole)

Shanfeng Wang,† Peiying Guo,‡ Pingping Wu, and Zhewen Han*

Key Laboratory for Ultrafine Materials of Ministry of Education, School of Materials Science and Engineering, East China University of Science and Technology, Shanghai 200237, China

Received January 26, 2004; Revised Manuscript Received March 22, 2004

ABSTRACT: New rod−coil copolymers based on poly(*p*-phenylene benzobisoxazole) (PBO) have been synthesized and characterized to explore a new ordered molecular structure at the supramolecular level for regulating photophysical properties and obtaining new blue light-emitting materials. The microstructure and physical properties of such rod−coil copolymers, poly(1,4-phenylenebenzobisoxazole-*co*-octamethylenebenzobisoxazole) (PBO−PBOC8), were determined by FTIR, ^{1}H NMR, viscometry, WAXD, and TGA. The chain flexibility and photophysical properties of copolymers can be efficiently modulated by the copolymer composition while the structure remains ordered, which is quite different from their analogue: the amorphous rod−coil copolymers poly(1,4-phenylenebenzobisthiazole-*co*-decamethylenebenzobisthiazole) (PBZT−PBTC10) reported by Jenekhe et al. [*J. Am. Chem. Soc.* **1995**, *117*, 7389]. Photophysical properties of these polymers both in methanesulfonic acid (MSA) and in the solid state were investigated in detail using UV absorption, photoluminescence (PL) spectroscopy, and time-resolved PL spectroscopy to reveal the relation between the morphology and photophysical properties. The PL peak of the rod−coil copolymers was greatly blue-shifted from that of the pure conjugated polymer PBO, particularly at rod molar fractions of less than 0.5. Furthermore, electronic paramagnetic resonance (EPR) studies of the paramagnetic defect in the copolymers were performed to explore the effect of structural change on the EPR signal.

Introduction

Conjugated polymers have attracted considerable attention from the scientific community for being used in electronics, optoelectronics, and nonlinear optics.[1,2] The discovery[3] that conjugated polymers could be used in organic light-emitting diodes (OLEDs) has provided motivation for achieving commercial applications in the display technology market. Although conjugated polymers have made extraordinary progress, some challenges remain for obtaining high-efficiency, high-durability emitting components in the pure blue spectral region.

Photophysical properties of conjugated polymers are important for understanding both the nature of their excited states and the operation of electroluminescent devices. The electronic properties of conjugated polymers depend strongly on the conformation of the polymer chains and the chain packing in the solid state.[4] It is well accepted that emission in interchain excitons results in suppressed luminescence quantum efficiency.[4−12] Many studies have suggested means to control the degree of interchain excitons by decreasing the intermolecular interactions by introducing bulky side groups to the conjugated backbone or blending two different components.[13−16] Moreover, since one particular advantage of conjugated polymeric materials is the possibility of chemical tailoring to realize desired properties, the energy gap of conjugated polymers may be tuned by chemical substitution or copolymerization.[14,17]

Scheme 1

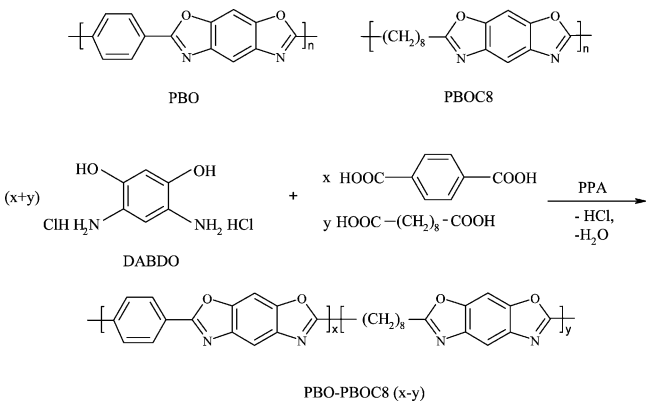

As a result of great interest in the optically and electronically active properties of the highly conjugated and rigid-rod-like molecules, a variety of oligomers and polymers have been synthesized to establish the molecular structure and property relationship.[14,18] In addition to molecular structure, supramolecular structure was reported to have a dramatic effect on the physical properties of conjugated rodlike molecules.[19−21] Thus, manipulation of supramolecular structure in conjugated rods is of great importance to achieve efficient optophysical properties in solid-state materials. One way to manipulate the supramolecular structure might be incorporation of the conjugated rod into a rod−coil molecular architecture which would allow formation of well-defined one-, two-, or three-dimensional conjugated domains in nanoscale dimensions.[21]

As described in Scheme 1, polybenzazoles such as poly(*p*-phenylene benzobisoxazole) (PBO) and poly(*p*-phenylene benzobisthiazole) (PBZT) have many out-

† Present address: Department of Polymer Science, University of Akron, Akron, OH.
‡ Equal contribution as the first author.
* Corresponding author: Tel +8621-64253060; fax +8621-64233269, e-mail zhwhan@ecust.edu.cn.

10.1021/ma0498316 CCC: $27.50
Published on Web 04/22/2004

standing photoluminescence properties as well as mechanical properties and thermal stability.[11−13,17,22−25] Poly(benzazole)s are favorably considered to be superior electron-transport and hole-blocking materials in polymer LEDs.[26] Thin film transistors with relatively high mobility have been made from PBZT and PBZT blends.[27] Previously, the rod−coil copolymers poly(1,4-phenylenebenzobisthiazole-*co*-decamethylenebenzobisthiazole) (PBZT−PBTC10) consisting of these electroactive and photoactive segments were synthesized for comparison with their homopolymer PBZT.[17] The luminescence quantum yield varied with copolymer composition, reaching an enhancement of over 6-fold compared to the "bulk" pure conjugated polymer PBZT with the formation of nanocomposites.[17] Previously, it was also reported that poly(benzazole)s had significant electron paramagnetic resonance (EPR) signals, and the soliton−antisoliton model was established to explain the EPR signal in such polymers.[28]

In this paper, we report the synthesis, characterization, photophysical properties, and paramagnetic properties of the rod−coil copolymers poly(1,4-phenylenebenzobisoxazole-*co*-octamethylenebenzobisoxazole) (PBO−PBOC8) to contrast with the previous rod−coil copolymer PBZT−PBTC10 in terms of the interplay between morphology and photophysical properties. A series of copolymers with different rod−coil composition ratios *x*:*y*, shown as PBO−PBOC8 (*x*−*y*), have been prepared to allow studies of structure−property relationships in this class of polymers. The molecular structures of the rod−coil copolymer PBO−PBOC8 together with its homopolymers PBO and PBOC8 are shown in Scheme 1. The UV−vis absorption, excitation, and emission spectra of these polymers are reported. At the end of this paper, EPR spectroscopy studies are described to investigate how structural change affects paramagnetic properties of these copolymers.

Experimental Section

Synthesis. As shown in Scheme 1, in the synthesis of PBO−PBOC8 (2−8), 2,4-diamino-1,5-benzenediol (DABDO) dihydrochloride (3.20 g, 15 mmol) was dissolved in 46.26 g of deaerated 80.8% PPA (poly(phosphoric acid)). The reaction vessel was purged with argon. After dehydrochlorination at 80 °C under vacuum, the reaction vessel was cooled to 50 °C; 0.5 g (3 mmol) of TPA (terephthalic acid) and 2.43 g (12 mmol) of SA (sebacic acid) were added together with 14.49 g of fresh P_2O_5. The reaction temperature was gradually raised to 100 °C for 4−6 h, then to 140 °C for 6 h, and finally to 180 °C and held for 12 h. The highly viscous polymerization solution (yellow in color) in PPA was precipitated in water and purified by extraction of PPA with water for 2−3 days. The polymer was desiccated at 60 °C in a vacuum oven. Thin films of good optical quality were prepared using Jenekhe's method,[29,30] i.e., spin-coating of the polymer solution in nitromethane/$AlCl_3$ with a polymer concentration of about 3 wt % onto silica substrates. The thin films were dried at 80 °C in a vacuum oven for 12 h after complete decomplexation in deionized water for over 3 days. Intrinsic viscosity $[\eta]$ = 5.1 dL/g (30 °C in methanesulfonic acid). ^{1}H NMR (D_2SO_4, ppm): δ = 2.0−2.4 (8H), 2.6 (4H), 4.0 (4H), 8.9−9.0 (2H), 9.1 (2H), 9.2 (2H), 9.3−9.4 (4H). FTIR (free-standing film, cm^{-1}): 2931, 2854, 1626, 1584, 1527, 1495, 1462, 1412, 1365, 1135, 1111, 1060, 874, 725, 704.

The synthesis of the other copolymers was similar, except the different ratio of TPA to SA. The ^{1}H NMR resonances and FTIR bands of the other copolymers were identical to those of PBO−PBOC8 (2−8).

Characterization. Intrinsic viscosities $[\eta]$ of all the polymers were measured in methanesulfonic acid (MSA) at 30 °C by using a modified device based on a Ubbelohde capillary viscometer.[31] MSA was obtained from Sigma-Aldrich Chemical Co. Thermogravimetric analysis (TGA) was done using a Du Pont model 951 thermal analyst. The TGA data were obtained in flowing nitrogen at a heating rate of 10 °C/min. FTIR spectra were taken at room temperature using a Nicolet Magna-IR 550 Fourier transform infrared (FTIR) spectrometer. The ^{1}H NMR spectra of the polymer solutions in D_2SO_4 were obtained at 500 MHz using a Bruker DMX-500 instrument.

Optical absorption spectra of thin films and the polymer solutions were obtained with a Varian Cary 500 UV−vis−near-IR spectrophotometer and a Unico UV-2102 PCS spectrophotometer, respectively. Photoluminescence spectra of polymer/MSA solution were recorded on a Varian Cary Eclipse fluorescence spectrophotometer at room temperature. Photoluminescence (PL) spectra of copolymer films were recorded on an Edinburgh fluorescence spectrophotometer at room temperature. Time-resolved photoluminescence decay measurements were performed by using the time-correlated single photon counting (SPC) technique—the Edinburgh Lifespec-ps equipped with a pulsed diode laser 80-B, which was operated at 40 MHz, and a MCP−PMT detector. The samples were excited at 370 nm.

Wide-angle X-ray diffraction (WAXD) curves of copolymers were obtained on a Rigaku D/max-rB automated powder diffractometer. The instrument was set up with a Cu Kα (λ = 0.154 056 nm) X-ray source operating at 40 kV and 100 mA. The 2θ scan range was set to be 3°−50°.

A Hitachi ER-200D EPR spectrometer was used in the EPR studies. The resonance frequency was 9.7735 GHz, and the modulating frequency was 100 kHz. Quantitative EPR measurements were monitored by comparison to a ruby standard with a spin concentration of about 2.6 × 10^{18} spins/g.

Table 1. Physical Properties of PBO, PBOC8, and Their Copolymers

polymer	intrinsic viscosity $[\eta]^a$	thermal stability (°C)^b
PBO	24.5	673
PBO−PBOC8 (8−2)	4.8	492
PBO−PBOC8 (6.5−3.5)	6.1	481
PBO−PBOC8 (5−5)	3.1	466
PBO−PBOC8 (4−6)	6.8	466
PBO−PBOC8 (3−7)	5.8	471
PBO−PBOC8 (2−8)	5.1	462
PBOC8	6.5	457

[a] In MSA at 30.0 ± 0.2 °C. [b] Onset of thermal decomposition in N_2 at 10 °C /min.

Results and Discussion

Intrinsic Viscosity and Thermal Stability. Table 1 lists the properties of the polymers. The thermal stability of rod−coil copolymers is much lower than that of PBO in the high-temperature range, though it has been enhanced compared to the flexible-coil polymer PBOC8. There was more residual left for copolymers with higher rod composition when the temperature arrived at 600 °C. TGA results are expected and consistent with the earlier conclusion that the thermal stabilities of the copolymers are largely limited by the methylene groups in the backbone.[17] Nevertheless, the copolymers have reasonably good thermal stability with the onset decomposition temperature of 457−492 °C.

Morphology. All the WAXD patterns of the copolymers shown in Figure 1a have two major diffraction peaks at the interplanar spacing corresponding to around 2θ = 16° (~0.55 nm, labeled as peak A) and 22° (~0.40 nm, labeled as peak B). The periodicity for peak A stands for the side-to-side distance between two neighboring polymer chains. For PBO, its side-to-side distance is 0.55 nm (2θ = 16°), corresponding to the

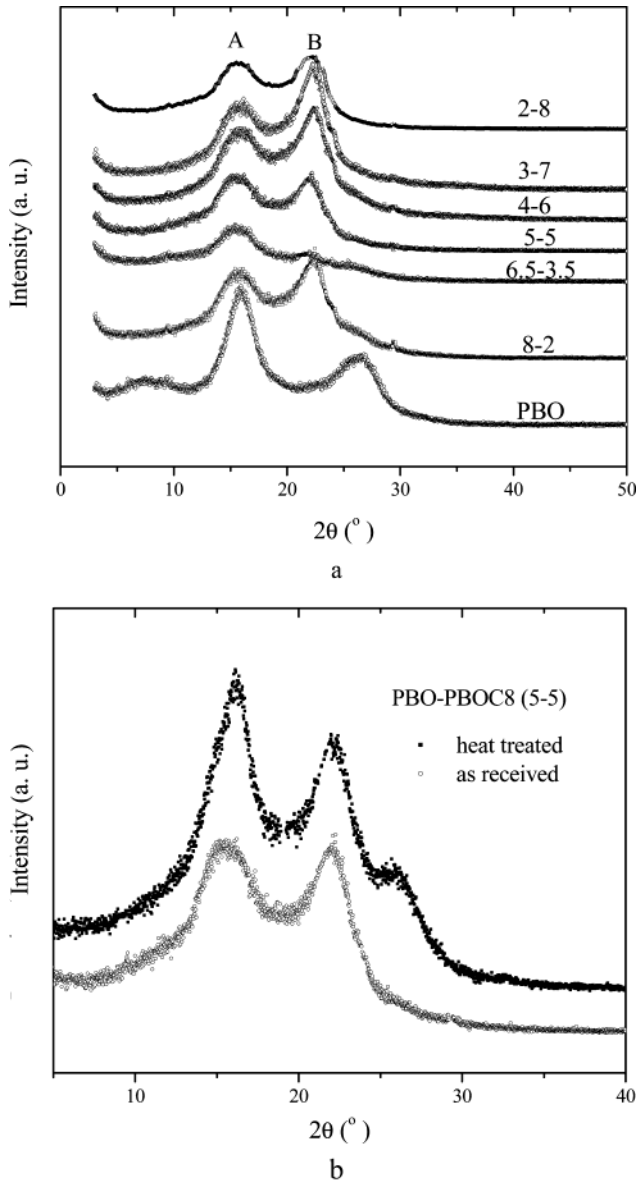

Figure 1. Wide-angle X-ray diffraction patterns of (a) PBO−PBOC8 copolymers and PBO and (b) PBO−PBOC8 (5−5) samples after heat treatment at 350 °C for 10 min and without heat treatment.

(200) plane.[34] The side-to-side distance does not change for all the polymers with various rod composition. The diffraction peak B at $2\theta = 22°$ for all the copolymers shown in Figure 1a stands for the face-to-face distance between two neighboring polymer chains. The face-to-face distance for PBO is 0.336 nm ($2\theta = 26.5°$), corresponding to the (010) plane.[32] As depicted in Figure 1a, there is a clear shift in peak B when the coil segments were introduced to the PBO chain, indicating a significant increase in the face-to-face distance for copolymers because the flexible segments affect the rigid-chain ordered structure of PBO. Although the peaks of copolymers are slightly broader than that of PBO, the ordered structures of copolymers are still similar to that of PBO with identical side-to-side distances and larger face-to-face distances. The morphology here is quite *different* from the results in Jenekhe's report[17] on PBZT−PBTC10, in which the crystalline peaks characteristic of either the rodlike or coillike homopolymers could not be detected, and the disordered morphology was reported. The remained ordered or semiordered

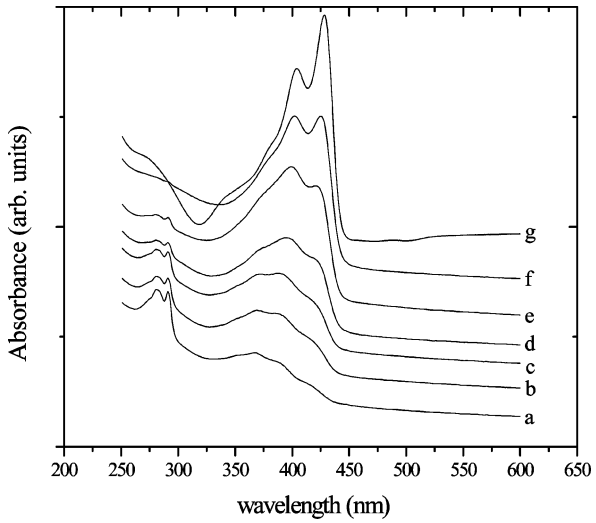

Figure 2. Absorption spectra of PBO and PBO−PBOC8 copolymers in MSA at 0.000 44 g/dL (a: PBO−PBOC8 (2−8); b: PBO−PBOC8 (3−7); c: PBO−PBOC8 (4−6); d: PBO−PBOC8 (5−5); e: PBO−PBOC8 (6.5−3.5); f: PBO−PBOC8 (8−2); g: PBO).

structure indicates that the coillike segment length, i.e., the number of methylene group in the rod−coil copolymers, can regulate not only the flexibility of the polymer chain but also the morphology and chain packing. The disordered nature of these copolymers, at $f < 0.5$, arises from the random distribution of rods of different lengths in the matrix of the flexible coil. Therefore, all the three morphologies demonstrated in Figure 1 in ref 17 can be achieved by designing and synthesizing such rod−coil copolymers with different coil segment lengths.

Figure 1b shows the effect of heat treatment on the molecular structure of the copolymer PBO−PBOC8 (5−5). After heat treatment at 350 °C for 10 min, the chain regularity and the conjugation length in these polymers were improved, and the packing of the polymer chains became more compact, reported similarly for poly(2,5-benzoxazole) (ABPBO), poly(2,5-benzothiazole) (ABPBT),[33] and the copolymer PBO−ABPBO.[34] As shown in Figure 1b, the intensities of the peaks increase significantly, and the half-peak width of the peaks decreases after heat treatment, which means that the regularities in side-to-side direction and face-to-face direction of those polymer chains were enhanced efficiently by heat treatment. Moreover, a new broad peak characteristic of PBO face-to-face distance shows up at $2\theta = 26°$, indicating the ordered structure was also improved in rod segments upon heat treatment.

Absorption Spectra. Figure 2 shows the optical absorption spectra of the copolymers and PBO solutions in MSA at a concentration of 0.000 44 g/dL. There are two groups of peaks in the absorption spectra of copolymers in the 270−300 and 350−450 nm range. The coillike nonconjugated polymer PBOC8 and consequently the coillike segments of the copolymers do not absorb in the 340−600 nm spectral range, meaning that the absorption peaks in this spectral range largely reflect the conjugated rodlike segments in the copolymers. The two peaks of copolymers in the 350−450 nm range are slightly blue-shifted from those of PBO (at 405 and 429 nm), and the peak intensity progressively decreases with increasing coil composition. Another group of peaks in the 270−300 nm range should be attributed to the coillike segments in the copolymers

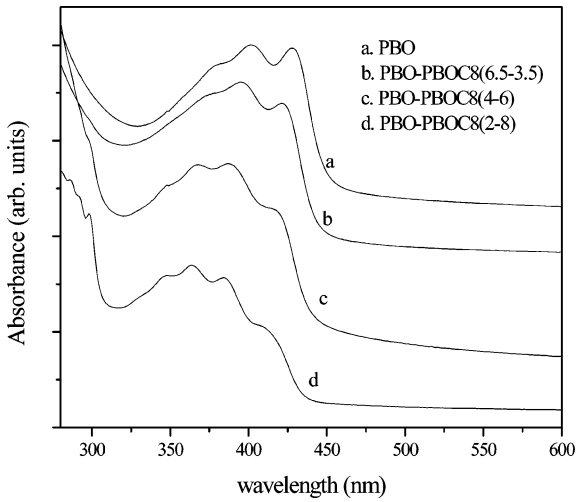

Figure 3. Absorption spectra of PBO and PBO−PBOC8 copolymer thin films.

since there is no significant peak in the absorption spectrum of PBO in this range, and the peak intensity progressively increases with increasing coil composition in the copolymers.

Figure 3 shows the absorption spectra of the copolymers and PBO thin films, mainly reflecting the conjugated segments in the copolymers. Similar to the spectra of PBZT−PBTC10,[17] a structured spectrum with five overlapped peaks can be observed for PBO−PBOC8 (2−8) in the 320−440 nm region. At higher rod compositions, spectra with similar line shape can be seen in Figure 3 (as curves b−d), and the peaks at lower wavelengths merge as the two major peaks in curve a. Same as the change in the absorption spectra in the solutions in Figure 2, the absorption spectra for copolymer thin films are also progressively red-shifted with increasing the rod composition. Compared with the absorption spectra of PBZT−PBTC10,[17] the vibronic peaks for the homopolymer PBO are discernible at a lower rod composition in PBO−PBOC8 copolymers because the shorter nonconjugated segments C8 other than C10 in PBZT−PBTC10 are used presently.

As indicated in ref 17, two important effects of *chromophore size* and *spatial confinement* of the chromophores can be observed for PBZT−PBTC10 when the rod composition is low, and the conjugated segments with reduced chromophore size can be considered as diluted or confined in the nonconjugated matrix. In the present study, such effects can also be verified using the composition-dependent absorption spectra of PBO−PBOC8 in Figure 3. Both the absorption peaks and edge shift to higher energy when the rod composition decreases, and the structured spectrum shows up for PBO−PBOC8 (2−8) finally.

Photoluminescence Spectra. The PL spectra of copolymers in MSA at the concentration of 0.000 44 g/dL are shown in Figure 4. It can be observed that the composition-dependent excitation spectra (Figure 4a) for copolymers in MSA are similar to the absorption spectra in Figure 2. When the rod composition is 0.8, a broad, strong peak can be observed in the 340−440 nm range, and such an excitation peak is blue-shifted slightly with increasing coil composition. The peaks in another spectral range (275−300 nm) start to show up when $f < 0.5$, and the position of the peaks does not change obviously with composition. As shown in the UV spectra of the copolymers and PBO in MSA in Figure 2, the

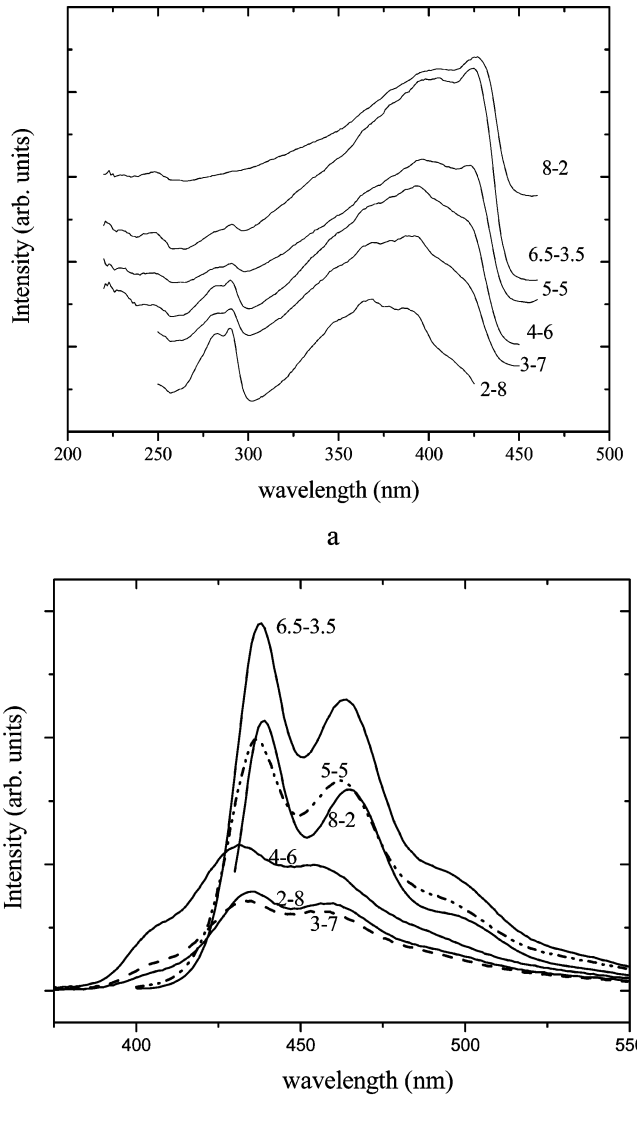

Figure 4. Photoluminescence (a, excitation; b, emission) spectra of PBO−PBOC8 copolymers in MSA at 0.000 44 g/dL.

excitation peaks at the longer and shorter wavelengths reflect the rodlike and coillike segments in the copolymers, respectively.

The emission spectra shown in Figure 4b of copolymers in MSA at 0.000 44 g/dL are nearly mirror images of the absorption spectra in Figure 2. The emission curves contain two major peaks with a well-resolved vibronic stucture. Meanwhile, the emission peaks are all blue-shifted, and the difference of the two peaks decreases with the coil composition, especially when f is less than 0.5. This result is expected, considering that the coplanarity of protonated PBO rigid chain in the dilute solutions is much better than that of PBOC8 because the flexible components may deteriorate both the conjugation length in PBO and the coplanarity of the polymer chain in dilute solutions.

The steady-state PL spectra of copolymers were measured in order to investigate the effects of the rod−coil copolymer composition and supramolecular structure on the solid-state PL. The emission spectra of copolymers (6.5−3.5, 4−6, 3−7, and 2−8) and PBO are shown in Figure 5, and the data of the PL spectra are listed in Table 2. As expected, the emission spectra of copolymers are blue-shifted obviously from that of PBO,

Table 2. Photoluminescence Data of Solid State PBO and PBO−PBOC8 Copolymers

	PBO[c]	PBO−PBOC8 (6.5−3.5)	PBO−PBOC8 (4−6)	PBO−PBOC8 (3−7)	PBO−PBOC8 (2−8)
ex[a] (nm)	415	381	372	369	327
intensity	2100	3000	2600	2100	2100
em[b] (nm)	544	488	486	470	469
intensity	4000	6300	6200	5900	4900

[a] Excitation wavelength. [b] Emission wavelength. [c] Measured using a different instrument.

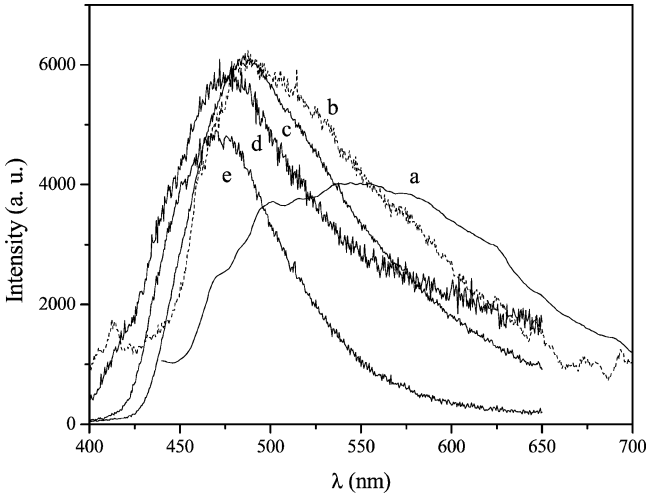

Figure 5. Photoluminescence emission spectra of solid-state PBO−PBOC8 copolymers and PBO (a: PBO; b: PBO−PBOC8 (6.5−3.5); c: PBO−PBOC8 (4−6); d: PBO−PBOC8 (3−7); e: PBO−PBOC8 (2−8)).

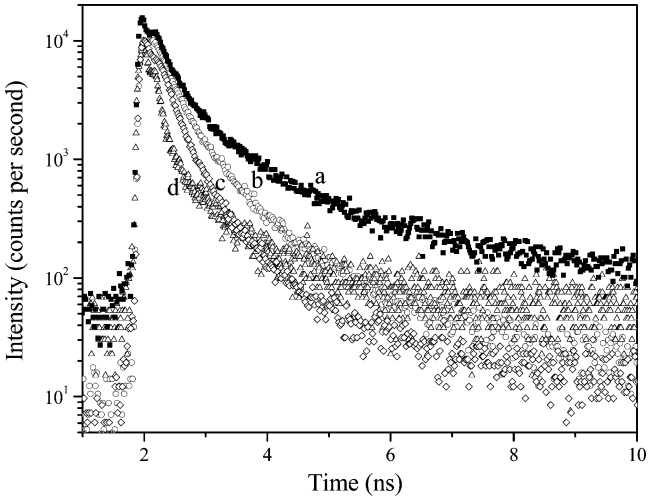

Figure 6. Time-resolved PL decay dynamics of copolymers (a: PBO; b: PBO−PBOC8 (4−6); c: PBO−PBOC8 (3−7); d: PBO−PBOC8 (2−8)).

Table 3. Time-Resolved PL Decay Dynamics Parameters for Copolymers Excited at λ = 370 nm

sample	τ_1, ns (%)	τ_2, ns (%)	λ_{det}, nm
PBO	0.24 (46.75)	1.11 (53.25)	550
PBO−PBOC8 (4−6)	0.35 (70.09)	1.42 (29.91)	470
PBO−PBOC8 (3−7)	0.19 (83.40)	1.99 (16.60)	470
PBO−PBOC8 (2−8)	0.29 (77.66)	1.30 (22.34)	470

which are also consistent with the result of copolymer/MSA solutions. The emission peaks of copolymers all locate in the region of blue light (440−495 nm), and the feature is much narrower than that of PBO. Because the thin film PL spectra of PBO and copolymers are tested using different instruments, a comparison of PL emission intensity may not be valid. Nevertheless, the results presented here indicate that (1) blue luminescence materials can be efficiently obtained by tuning the copolymer composition and (2) enhanced quantum efficiency is expected considering the reduction of aggregate formation due to the effect of *spatial confinement* of chromophores, which was also indicated in the studies on PBZT−PBTC10.[17]

The variations of the emission peak wavelength λ_{max} with copolymer composition are listed in Table 2; the emission spectra of films are red-shifted compared with those of solutions, and a larger Stokes shift $\Delta\lambda_{max}$ between absorption and emission maxima can be observed in the film spectra. Moreover, the emission and excitation spectra of solid-state copolymers are broad and structureless compared with those of the solutions. Jenekhe and Osaheni proposed that excimer emission accounts for the large $\Delta\lambda_{max}$ in conjugated polymers and rod−coil copolymers.[11,17] As can be seen from the figures and tables listed, the Stokes shift increases with the rod composition, and the tendency is more obvious when $f > 0.5$. The most plausible reason for the Stokes shift variation in copolymers is the variation in the *spatial confinement* effect; that is to say, the existence of coillike segments has broken the continuity of rodlike segments and separated the conjugated segements from each other to avoid strong interactions. When the rod composition increases, a more coplanar conformation can be more easily formed, and the interchain excitons consequently result in a red-shifted emission. The planar structures suggest that in the solid state molecules may orient in a π-stacked configuration, which results in the strong π-interactions existing between an excited benzoxazole chromophore and the surrounding benzoxazole chromophores in the solid state.[11] Blatchford et al.[7] have investigated the spectra of film and powder of pyridine-based polymers, contrasting to film the powder spectrum closely resembles the solution result, indicating that aggregate formation is morphology-dependent. In addition, the methods of film casting would also result in the red shift of spectra. Therefore, it is also a possible origin of the red shift in film spectra presented in this paper that nitromethane as a component of solvent evaporates rapidly in the fabrication of the thin films.

Luminescence Lifetime Measurements of Solid-State Copolymers. Typical copolymer PL decay dynamics are shown in Figure 6, and the best fit of two lifetimes with their amplitudes for each copolymer are given in Table 3. All the experiments were performed at room temperature with 370 nm excitation, and the decay of the PL was collected at various wavelengths shown as λ_{det} in Table 3.

As shown in Figure 6, the PL decay dynamics of the copolymers improved progressively from PBO−PBOC8 (2−8) to the homopolymer PBO. The multiple lifetimes needed to describe the PL decay dynamics of the copolymers suggest the existence of more than one excited-state species or the occurrence of various excited-state processes. The luminescence lifetimes of PBO−PBOC8 (3−7) and PBO−PBOC8 (2−8) are 0.19 and 0.29

Table 4. EPR Parameters of the Samples Considered Herein at Room Temperature

parameter	PBO[28]	PBO−PBOC8 (8−2)	PBO−PBOC8 (6.5−3.5)	PBO−PBOC8 (5−5)	PBO−PBOC8 (4−6)	PBO−PBOC8 (3−7)	PBO−PBOC8 (2−8)
g	2.0036	2.0034	2.0034	2.0037	2.0036	2.0037	2.0039
ΔH_{pp} (G)	7.2	7.1	7.4	7.3	8.9	8.1	8.6
A/B	1.06	1.26	1.25	1.23	1.14	1.24	1.17
N_s ($\times 10^{15}$ spins/g)	0.5[a]	3300	3800	4600	2100	2000	380

[a] The samples were monitored by comparison to a diamond standard in ref 28.

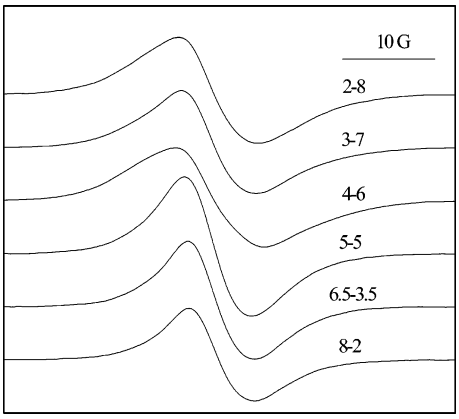

Figure 7. EPR spectra of PBO−PBOC8 copolymer films, as-received.

ns, and the decay profiles (curves c and d in Figure 6) follow a single-exponential profile with an amplitude of ~80%. The PL decay dynamics is similar to the results for PBO/MSA solutions, which showed a single-exponential decay with a lifetime of ~0.3 ns.[12] In these cases, the fast decay of the solution-like emission suggests rapid diffusion of excitons to aggregates sites that is facilitated by Förster transfer because of the strong overlap of intrachain emission and aggregate emission.[7,35] When the rod composition is around 0.5, the decay profile (curve b in Figure 6) can still be described using a single-exponential decay profile with an amplitude of ~70%. The luminescence dynamics of PBO thin film exhibited to be nonexponential and two lifetimes with similar amplitude were resolved, which were also reported previously.[12,13] The long-lived component (~1 ns) in the PL decay of PBO thin film is due to the aggregate emission since the longer radiative lifetime indicates a lower probability for radiative decay.

The time-resolved PL results here are consistent with the earlier report for PBZT−PBTC10,[17] in which the PL decay dynamics of the copolymers improved progressively from a nonexponential decay mechanism in PBZT−PBTC10 (8−2) to a largely single-exponential decay in PBZT−PBTC10 (2−8). The comparison between PBO−PBOC8 and PBZT−PBTC10 shows that the *spatial confinement* effect can be also observed in the ordered chain packing structure with greater face-to-face interchain distance in PBO−PBOC8. Such an effect suppresses the possibility of chromophore aggregation and brings about the solution-like PL decay dynamics, which consequently enhances the PL quantum efficiency.

EPR Studies. Figure 7 shows that the rod−coil copolymers presented here are paramagnetic, and the spin concentrations are sufficiently high (3.8×10^{17}−4.6×10^{18} spins/g) to suggest that the paramagnetic centers are intrinsic. As reported previously,[28] there is no EPR signal in DABDO dihydrochloride, one monomer for synthesizing poly(benzobisoxazole)s, while the model compounds with limited numbers of conjugation also have EPR signals. The typical EPR signal of the copolymers in Figure 7 is a Lorentzian single line without resolved hyperfine splitting, which is consistent with the results for other polybenzazoles.[28]

In the previous report,[28] we ascribed the EPR signals in polybenzazoles to the existence of soliton and antisoliton, which is well accepted as the origin of EPR signal in conjugated polymers.[36] In PBO−PBOC8, the two resonance structures of the phenyl ring or heteroring are not degenerate, and the defects exist in the boundary nitrogen atom in pairs: soliton−antisoliton, as illustrated in Figure 8.

The main results of the EPR studies, including electron Zeeman g-factor, peak-to-peak line width ΔH_{pp}, asymmetry parameter A/B defined by the ratio the left peak height A and right peak height B, and spin concentration N_s, are summarized in Table 4. It should be noted that the two EPR quantitative measurements were performed on different spectrometers with different standards (a ruby standard presently and a diamond standard in previous paper[28]). The spin concentrations obtained for rod−coil copolymers are much larger than the values reported previously[28] for PBO and copolymers PBO−ABPBO by 3−4 orders in magnitude. Then the spin concentrations for copolymers in the present study are on the same order with other conjugated polymers such as poly(*p*-phenylene) (PPP) (~10^{18} spins/g),[37] and those values correspond to one unpaired spin per 390−3600 average repeating conjugated units. As shown in Table 4, the spin concentration N_s does not change much with copolymer composition when $f > 0.5$; however, N_s drops dramatically by 1 order when $f < 0.5$ because the origin of the EPR signal is in conjugated segments while nonconjugated segments efficiently retard soliton transport. The phenomenon that the spin concentration was influenced by copolymer composition

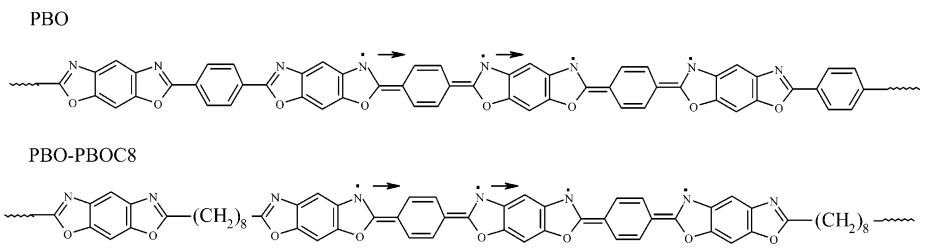

Figure 8. Schematic representations of hypothetical soliton−antisoliton in PBO and PBO−PBOC8.

only when $f < 0.5$ agrees with the conclusion[28] that the average conjugation length for intrinsic paramagnetic properties is no more than 2 repeat units, and the phenyl ring plays a vital role in transporting soliton as suggested in Figure 8.

The average *g*-factors for PBO−PBOC8 varying from 2.0034 to 2.0039 are in contrast to a typical isotropic *g*-factor of 2.0023 observed for *trans*-polyacetylene (PA)[38] or 2.0025 for PPP,[37] which is equal to the free electron value. The *g*-factor shift of around 10^{-3} originates from the radical localized on or near a heteroatom, such as oxygen in carboxylic species or nitrogen in pyridines.[39]

The line widths of EPR spectra, ΔH_{pp}, for the PBO and rod−coil copolymers range from 7.0 to 9.0 G approximately. Compared with 1.46 G for *trans*-PA[40] and 0.67 G for poly(thiophene),[41] the ΔH_{pp} for heteroatom-centered conjugated polymers such as poly(benzobisoxazole)s[28] and poly(phenylene sulfide)[42] and rod−coil copolymers here are rather large, suggesting weaker delocalization of unpaired electrons on the conjugated polymer chain. Moreover, transport through nitrogen is predicted to be somewhat retarded relative to carbon, and oxygen or sulfur is not expected to participate in the π-conjugation.[43] It can be seen in Table 4 that the line width tends to be broader with increasing coil composition, and the change is more significant when the coil composition is below 0.5. One reason is that the degree of structural disorder increases with increasing coil composition. The studies of polypyrrole by Scott et al.[44] imply that a system having a considerable amount of disorder leads to the possibility of inhomogeneous broadening through a distribution of *g*-factors. On the other hand, the increase of coil composition results in the decrease of the conjugation length, and then the spin centers are expected to be delocalized over less conjugation units, which consequently will result in the broadened EPR spectra. So the line width change of the copolymers is the combined result of structure disorder and reduced conjugation length.

From Figure 7 and the data in Table 4, the copolymer films show a slight asymmetry with the asymmetry parameter *A*/*B* ranging from 1.17 to 1.28. EPR spectra of conduction electrons in metals exhibit a Dysonian line shape, provided the dimensions of the sample are large in comparison to the skin depth.[45] Generally the shape of the conducting polymers is Lorentzian but slightly asymmetric. Because of the very small thickness, low conductivity of the samples, and the persistence of asymmetry to low temperature, this asymmetry could also result from anisotropy of an inhomogeneous distribution in the *g*-factor.[44]

Conclusions

In summary, we have synthesized and characterized new rod−coil blue-emitting copolymers based on PBO rodlike segments to make a comparison with their amorphous analogues PBZT−PBTC10 reported in ref 17. We have also studied the photophysical properties of these polymers, including thin films on the silicate substrate and solutions in methanesulfonic acid (MSA). The results show that the introduction of coillike segments into PBO makes the UV spectra and photoluminescence spectra blue-shifted from that of conjugated homopolymer PBO while the morphology of the copolymers remains ordered with a greater face-to-face interchain distance. Similar to the previous report on PBZT−PBTC10, the PL decay measurements showed single-exponential decay dynamics when the rod composition in copolymers is less than 0.5 due to the *spatial confinement* effect. EPR studies of the paramagnetic defect in the copolymers further proved that the introduction of coillike segments into PBO results in broadening line width and lowering spin concentration when the rod composition is lower than 0.5. Together with the report on PBZT−PBTC10 in ref 17, the ordered, semi-ordered, and disordered chain structures can be achieved by designing and synthesizing such rod−coil copolymers. Moreover, the interplay between the morphology and photophysical properties can be investigated on the basis of such a scheme.

Acknowledgment. This research was supported by the "863" project of the National Science and Technology Department of China. The number of the financial item is 2002AA305109.

Supporting Information Available: FTIR, ^{1}H NMR, and TGA spectra of the copolymers, tables of data in WAXD patterns (Figure 1), absorption spectra (Figures 2 and 3), and photoluminescence spectra (Figure 4). This material is available free of charge via the Internet at http://pubs.acs.org.

References and Notes

(1) Friend, R. H.; Gymer, R. W.; Holmes, A. B.; Burroughes, J. H.; Marks, R. N.; Taliani, C.; Bradley, D. D. C.; DosSantos, D. A.; Brédas, J. L.; Logdlund, M.; Salaneck, W. R. *Nature (London)* **1999**, *397*, 121.
(2) Heeger, A. J. *Solid State Commun.* **1998**, *107*, 673.
(3) Burroughes, J. H.; Bradley, D. D. C.; Brown, A. R.; Marks, R. N.; Mackay, K.; Friend, R. H.; Burns, P. L.; Holmes, A. B. *Nature (London)* **1990**, *347*, 539.
(4) Schwartz, B. J. *Annu. Rev. Phys. Chem.* **2003**, *54*, 141.
(5) Samuel, I. D. W.; Rumbles, G.; Collins, C. J. *Phys. Rev. B* **1995**, *52*, R11573.
(6) Blatchford, J. W.; Gustafson, T. L.; Epstein, A. J.; Vanden Bout, D. A.; Kerimo, J.; Higgins, D. A.; Barbara, P. F.; Fu, D. K.; Swager, T. M.; MacDiarmid, A. G. *Phys. Rev. B* **1996**, *54*, R3683.
(7) Blatchford, J. W.; Jesson, S. W.; Lin, L.-B.; Gustafson, T. L.; Fu, D. K.; Wang, H. L.; Swager, T. M.; MacDiarmid, A. G.; Epstein, A. J. *Phys. Rev. B* **1996**, *54*, 9180.
(8) Lemmer, U.; Heun, S.; Mahrt, R. F.; Scherf, U.; Hopmeier, M.; Siegner, U.; Gobel, E. O.; Müllen, K.; Bässler, H. *Chem. Phys. Lett.* **1995**, *240*, 373.
(9) Nguyen, T.-Q.; Doan, V.; Schwartz, B. J. *J. Chem. Phys.* **1999**, *110*, 4068.
(10) Jakubiak, R.; Collison, C. J.; Wan, W. C.; Rothberg, L. J.; Hsieh, B. R. *J. Phys. Chem. A* **1999**, *103*, 2394.
(11) Jenekhe, S. A.; Osaheni, J. A. *Science* **1994**, *265*, 765.
(12) Wang, S.; Wu, P.; Han, Z. *Macromolecules* **2003**, *12*, 4567.
(13) Osaheni, J. A.; Jenekhe, S. A. *Macromolecules* **1994**, *27*, 739.
(14) Kraft, A.; Grimsdale, A. C.; Holmes, A. B. *Angew. Chem., Int. Ed.* **1998**, *37*, 402.
(15) Nguyen, T.-Q.; Schwartz, B. J. *J. Chem. Phys.* **2002**, *116*, 8198.
(16) Kulkarni, A. P.; Jenekhe, S. A. *Macromolecules* **2003**, *36*, 5285.
(17) Osaheni, J. A.; Jenekhe, S. A. *J. Am. Chem. Soc.* **1995**, *117*, 7389.
(18) Segura, J. L.; Martin, N. *J. Mater. Chem.* **2000**, *10*, 2403.
(19) Kim, J.; Swager, T. M. *Nature (London)* **2001**, *411*, 1030.
(20) Cornil, J.; Beljonne, D.; Calbert, J. P.; Brédas, J. L. *Adv. Mater.* **2001**, *13*, 1053.
(21) Lee, M.; Cho, B.-K.; Zin, W.-C. *Chem. Rev.* **2001**, *101*, 3869.
(22) Wolfe, J. F. In *Encyclopedia of Polymer Science and Technology*, 2nd ed.; Mark, H. F., Kroschmitz, J. I., Eds.; Wiley: New York, 1988; Vol. 11, pp 601−635.
(23) So, Y.-H.; Zaleski, J. M.; Murlick, C.; Ellaboudy, A. *Macromolecules* **1996**, *29*, 2783.
(24) Osaheni, J. A.; Jenekhe, S. A. *Chem. Mater.* **1992**, *4*, 1282.
(25) Osaheni, J. A.; Jenekhe, S. A. *Chem. Mater.* **1995**, *7*, 672.
(26) Alam, M. M.; Jenekhe, S. A. *Chem. Mater.* **2002**, *14*, 4775.

(27) Babel, A.; Jenekhe, S. A. *J. Phys. Chem. B* **2002**, *106*, 6129.
(28) Wang, S.; Wu, P.; Han, Z. *Polymer* **2001**, *42*, 217. Guo, P.; Wang, S.; Wu, P.; Han, Z. *Polymer* **2004**, *45*, 1885.
(29) Jenekhe, S. A.; Johnson, P. O.; Agrawal, A. K. *Macromolecules* **1989**, *22*, 3216.
(30) Jenekhe, S. A.; Johnson, P. O. *Macromolecules* **1990**, *23*, 4419.
(31) Wang, S.; Bao, G.; Wu, P.; Han, Z. *Eur. Polym. J.* **2000**, *36*, 1843.
(32) Fratini, A. V.; Lenhert, P. G.; Resch, T. J.; Adams, W. W. *Mater. Res. Soc. Symp. Proc.* **1989**, *134*, 431.
(33) Wang, S.; Bao, G.; Lu Z.; Wu, P.; Han, Z. *J. Mater. Sci.* **2000**, *35*, 5873.
(34) Wang, S.; Wu, P.; Han, Z. *J. Mater. Sci.* **2004**, *39*, 2717.
(35) Pope, M., Swenberg, C. E., Eds. *Electronic Processes in Organic Crystals* Oxford University Press: NewYork, 1982.
(36) Skotheim, T. A., Ed. *Handbook of Conducting Polymer*; Marcel Dekker: New York, 1986; Vol. 2.
(37) Jones, M. B.; Kovacic, P.; Howe, R. F. *J. Polym. Sci., Polym. Chem. Ed.* **1981**, *19*, 235.
(38) Goldberg, I. B.; Crow, H. R.; Newman, P. R.; Heeger, A. J.; MacDiarmid, A. G. *J. Chem. Phys.* **1979**, *70*, 1132.
(39) Young, C. L.; Witney, D.; Vistnes, A. I.; Dalton, L. R. *Annu. Rev. Phys. Chem.* **1986**, *37*, 459.
(40) Bernier, P.; Rolland, M.; Linaya, C. *Polymer* **1980**, *21*, 7.
(41) Tourillon, G.; Gourier, D.; Garnier, P. *J. Phys. Chem.* **1984**, *88*, 1049.
(42) Kispert, L. D.; Files, L. A.; Frommer, J. E.; Shacklette, L. W.; Chance, R. R. *J. Chem. Phys.* **1983**, *78*, 4858.
(43) Forner, W.; Seel, M.; Ladik, J. *J. Chem. Phys.* **1986**, *84*, 5910.
(44) Scott, J. C.; Pfluger, P.; Krounbi, M. T.; Street, G. B. *Phys. Rev. B* **1983**, *28*, 2140.
(45) Feher, G.; Kip, A. F. *Phys. Rev.* **1955**, *98*, 337.

MA0498316